https://doi.org/10.5194/hess-2022-350
Preprint. Discussion started: 17 October 2022

Hydrology and Earth System Sciences
Discussions

Investigating the performance of Genetic Particle Filter in snow data assimilation across snow climates

Yuanhong You[a], Chunlin Huang[b], Jinliang Hou[b], Ying Zhang[b]

[a]College of Geography and Tourism, Anhui Normal University, Wuhu, 241002, China

[b]Northwest Institute of Eco-Environment and Resources, Chinese Academy of Sciences, Lanzhou, 730000, China

Corresponding author: Chunlin Huang, Key Laboratory of Remote Sensing of Gansu Province, Northwest Institute of Eco-Environment and Resources, Chinese Academy of Sciences, Lanzhou, Gansu, 730000, China. (huangcl@lzb.ac.cn)

https://doi.org/10.5194/hess-2022-350
Preprint. Discussion started: 17 October 2022

Hydrology and Earth System Sciences
Discussions

Abstract

With the aim of reducing the uncertainty of simulations, data assimilation methodology is increasingly being applied in operational purposes. This study aims to investigate the performance of genetic particle filter which used as snow data assimilation scheme, designed to assimilate ground-based snow depth measurements across different snow climates. We employed the default parameterization scheme combination within Noah-MP model as model operator in the snow data assimilation system. And the feasibility of genetic particle filter used as snow data assimilation scheme was investigated at different sites, at the same time, the impact of measurement frequency, particle number on the filter updating of the snowpack state were also evaluated. The results demonstrated that the genetic particle filter can be used as snow data assimilation scheme and obtain satisfactory assimilation results across different snow climates. We found the particle number is not the crucial factor to impact the filter performance and one hundred particles can sufficient to represent the high dimensionality of the point-scale system. The frequency of measurements can significantly affect the performance of filter updating and a dense ground-based snow observational data always can dominate the accuracy of assimilation results. Finally, we concluded that the genetic particle filter is a suitable candidate approach to snow data assimilation and appropriate for different snow climates.

1. Introduction

Understanding snowpack dynamics is of critical importance to water resource management, agricultural production, avalanche prevention in mountain area and flood prediction. The presence of seasonal snow cover has highly sensitivity to climate change and a great influence on hydrological cycle (Barnett et al., 2005; Takala et al., 2011). High snow surface albedo can reduce the shortwave radiation absorption remarkably and the energy exchange between the land surface and atmosphere will be adjusted (You et al., 2020). Moreover, the property of low thermal conductivity can insulate the underlying soil, whose temperature variability is severely reduced towards a stable condition (Zhang et al., 2005; Piazzi et al., 2019). Snowmelt is an important water resource and plays a critical role in water supply in terms of soil moisture, runoff, and groundwater recharge (Dettinger, 2014; Griessinger et al., 2016; Oaida et al., 2019). Consequently, succeeds in catching snow dynamics is crucial for snowmelt runoff, atmospheric circulation, and hydrological predictions.

Recently, a growing effort is aimed at investigating the potential of data assimilation (DA) scheme in consistently improving snow simulations and obtain the optimal posterior estimate of snowpack state (Bergeron et al., 2016; Piazzi et al., 2018; Smyth et al., 2020; Abbasnezhadi et al., 2021). Many different DA methodologies have been developed with distinct degree of complexity, certainly, various performance since diverse level of complexity. The sequential DA techniques

https://doi.org/10.5194/hess-2022-350
Preprint. Discussion started: 17 October 2022

including basic direct insertion, optimal interpolation schemes, Kalman filter and its variants and particle filter are widely employed in practical applications. The greatest strength of sequential DA technique is that the model state can be sequentially updated when observational data available (Piazzi et al., 2018). The basic direct insertion method simple replace the model predictions with observations when available on the assumption that the observation is perfect and model prior is wrong (Malik et al., 2012). However, this method possible result in model shocks due to physical inconsistencies among state variables (Magnusson et al., 2017). Although the optimal interpolation scheme takes into account the observational uncertainty, this method still has great limitations (Dee et al., 2011; Balsamo et al., 2015). More advanced are the Kalman filter and its variants, which are typical sequential DA techniques and most commonly used in various applications. The standard Kalman filter (KF) just can be used in linear dynamic models since it depends on the assumption of system linearity (Gelb, 1974). Ensemble Kalman filter (EnKF) was proposed by Evensen (2003), in this method, the Monte Carlo approach was used to approximate error estimates based on an ensemble of model simulations and this method does not require a model a model linearization. Precisely due to this advantage, the EnKF has been widely used in snow data assimilation. For example, the EnKF was employed to assimilate MODIS snow cover extent and AMSR-E SWE into hydrologic model to improve modeled SWE (Andreadis et al., 2005). The feasibility of assimilating fractional snow cover detected by MODIS into land surface model using EnKF was investigated, and the results show that the SWE estimates from the EnKF are most improved in various regions (Su et al., 2008). The impact of an EnKF-based assimilation of both ground-based SWE observations and snowfall and snowmelt rates on distributed SWE estimates was analyzed in Magnusson et al. (2014). More recently, three kinds of snow depth data which included the D-InSAR data retrieved from the remote sensing images, the automatically measured data using ultrasonic snow depth detectors, and the manually measured data were assimilated based on ensemble Kalman filter, and the results demonstrated that the assimilated snow depth data were spatiotemporally consecutive and integrated (Yang and Li, 2021). Although the EnKF was widely used in snow data assimilation and many studies generally stated that the EnKF has an excellent assimilation performance enabling to consistently improve snow simulations, some constraining limitations hinder filter performance (Chen, 2003). Firstly, this method was implemented at the assumption of model states follow gaussian distribution and just considers the first and second order moments, higher-order moments be ignored will makes relevant information be lost (Moradkhani et al., 2005). Unfortunately, the dynamic systems are usually strongly nonlinear and the involved probability distribution of state variables are not supposed to follow a Gaussian distribution (Weerts and El Serafy, 2006). Moreover, the filter performance was significantly affected by linear updating procedure in EnKF, and the state-averaging operations may be a huge challenge for highly complex models.

Particle filter (PF) is developed based on sequential Monte Carlo and widely used in snow data

https://doi.org/10.5194/hess-2022-350
Preprint. Discussion started: 17 October 2022

assimilation in recent years (Gordon et al., 1993). The greatest strength of PF scheme is free from the constraints of model linearity and error following Gaussian distribution, which makes the PF scheme suitable for nonlinear and non-Gaussian dynamic systems. This is also a significant advantage of PF over than other assimilation algorithms. Additionally, PF schemes give weights to individual particles but leave model states untouched, this makes PF more computationally efficient than ensemble Kalman filter and smoother (Margulis et al., 2015). An increasing interest focuses on applying PF scheme in snow data assimilation. For example, remotely sensed microwave radiance data was assimilated into snow model for updating model states by PF scheme, and the results demonstrated that the SWE simulations have great improvement (Dechant and Moradkhani, 2011). A newly PF approach proposed by Margulis et al. (2015) was used to improve SWE estimation through assimilating remotely sensed fractional snow-covered area. This technique was also implemented with the objective of obtaining high resolution retrospective SWE estimates over several Andean study basins (Cortes et al., 2016). PF scheme was also used to assimilate daily snow depth observations within a multi-layer energy-balance snow model, and result in an improvement of SWE and snowpack runoff simulations during the entire analysis period (Magnusson et al., 2017). Above studies generally state that the PF scheme is a well-performing data assimilation technique enabling to consistently improve model simulations. And either the assimilation of snow-related in-situ measurements or remotely sensed images through PF scheme succeeds in updating the predictions of snowpack dynamics. Nevertheless, particle degeneracy is the potential limitation for PF scheme, it occurs when the majority of particles have negligible weight and only a small number of particles with significant weights, such that the particles loss their ability to represent the state probability density function (Parrish et al., 2012; Abbaszadeh et al., 2017). Despite the resampling approach can effectively mitigate the particle degeneracy phenomenon, another potential limitation has been the sample impoverishment, that is, few particles have significant weight while most other particles with ignorable weight are abandoned during the resampling process, and the diversity of particles has been reduced. The Genetic Algorithm (GA) as an intelligent search and optimization method has been employed to mitigate the degeneracy and impoverishment problem (Kwok et al., 2005; Park et al., 2009; Mechri et al., 2014). GA is known as an effective approach to improve the performance of particle filter and has received more attention. For example, the crossover operator within GA was performed on the prior particles (Kwok et al., 2005). Mechri et al. (2014) implemented the genetic particle filter as data assimilation scheme and applied to land surface model which simulates prior subpixel temperature, the results demonstrated that GPF outperforms prior model estimations. However, few studies have used GPF as a snow data assimilation scheme. Certainly, in view of the promising performances of GPF assimilation scheme in snow data assimilation, this paper aims to investigate the potential of GPF in performing snow data assimilation, and the main goal of this research is to address the following issues: (1) Can the GPF be employed as a snow data assimilation

https://doi.org/10.5194/hess-2022-350
Preprint. Discussion started: 17 October 2022

scheme? (2) How is the assimilation performance of GPF in snow data assimilation across different snow climates? (3) The sensitivity of DA simulations to the frequency of the assimilated measurements and the particle number.

This paper is organized as follows. Section 2 describes the information of observation sites, snow module within Noah-MP model, GPF DA scheme, and DA experimental design. Experimental results are presented and discussed in Section 3. Section 4 summarizes the findings of this study.

2. Materials and methods

2.1 Study sites and data

With the consideration of the filtering performance maybe different under different environments, we selected eight seasonally snow-covered study sites with different snow climates in total in this study (Sturm et al., 1995; Trujillo and Molotch, 2014). These sites are distributed at different latitudes in the northern hemisphere, and the sites included the Arctic Sodankylä site (SDA, 179 m), located beside the Kitinen River in Finland and has a 2 m depths soil frost (Rautiainen et al., 2014); the Snoqualmie site (SNQ, 921 m) with a rain-snow transitional climate in the Washington Cascades of the USA, in this site, the snow depth measured from snow stakes was employed (Wayand et al., 2015); the maritime Col de Porte (CDP, 1330 m) site in the Chartreuse Range in the Rhone-Alpes of France; the Mediterranean climate Refugio Poqueira site (ROPA, 2510 m) in Sierra Nevada Mountains of Spain and has a high evaporation rate (Herrero et al., 2009); the Weissfluhjoch site (WFJ, 2540 m) in Davos of Switzerland, and automatic observations of snow depth were used in this study (Wever et al., 2015); the continental Swamp Angel Study Plot (SASP, 3370 m) site in the San Juan Mountains of Colorado, USA; and two sites from typical snow-covered regions in China, the Altay meteorological observation site (ATY, 735.3 m) in Northern Xinjiang, China, which has less wind in the winter season; the other one is the Mohe meteorological observation site (MOHE, 438.5 m) in a county of Northeast China, which is the northernmost part of China and has a cold temperate continental climate. Serially complete meteorological measurements are available and can be used as forcing data in these sites, certainly, the downward longwave and shortwave radiation values of MOHE were extracted from the China Meteorological Forcing Dataset (CMFD) (Chen et al, 2011), since there are no radiation measurements in this site.

It is noteworthy that the spatial variance on the performance of the model is negligible since these sites themselves are flat and surrounding vegetation types are uniform. We have used this data set to examine the sensitivity of snow depth to physics options, and the results showed that the dataset has a reliable quality, in addition, the location, detailed information of snow climates, and dataset process introduction of the eight sites can be also referenced in You et al. (2020a).

2.2 Snow module within Noah-MP model

The snow partial within Noah-MP model can be divided into three layers at most according to snow depth. When the snow depth $h_{snow} < 0.045$ m, the snowpack is combined with the top soil layer and there are no dependent snow layer exists. When $h_{snow} \geq 0.045$ m, the snow layer is created with the thickness equal to snow depth. When $h_{snow} \geq 0.05$ m, the snowpack will be divided into two layers and both thickness $\Delta z_{-1} = \Delta z_0 = h_{snow} / 2$. When $h_{snow} \geq 0.1$ m, the thickness of first layer is $\Delta z_{-1} = 0.05$ m and the thickness of second layer is $\Delta z_0 = (h_{snow} - \Delta z_{-1})$ m. When $h_{snow} \geq 0.15$ m, a third layer is created and the three thickness are: $\Delta z_{-2} = 0.05$ m and $\Delta z_{-1} = \Delta z_0 = (h_{snow} - \Delta z_{-2}) / 2$ m. When $h_{snow} \geq 0.45$ m, the layer thickness of the three snow layers are $\Delta z_{-2} = 0.05$ m, $\Delta z_{-1} = 0.2$ m, $\Delta z_0 = \left(h_{snow} - \Delta z_{-2} - \Delta z_{-1}\right)$ m. Certainly, the snow layer is combined with the neighboring layer since sublimation or melt, and be redivided depending on the total snow depth. The model provides an estimate of snow-related variables using energy and mass balance which computing process requires a series of meteorological forcing data: near surface air temperature, wind speed and direction, relative humidity, precipitation, air pressure, downward longwave and shortwave radiation. Snow accumulation or ablation parameterization of the Noah-MP model is based on the mass and energy balance of the snowpack, and the snow water equivalent can be calculated by following equation:

$$\frac{dW_s}{dt} = P_s - M_s - E . \tag{1}$$

Where W_s is the snow water equivalent, P_s is the solid precipitation, M_s is the snow ablation rate, E is the snow evaporation.

Due to the interception of snowfall by the canopy and subsequent sublimation from the canopy snow can greatly reduce the quantity of snow falling on the ground, a snow interception model was implemented into Noah-MP model. Within this model, the ground surface albedo is parameterized as an area-weighted average of albedos of snow and bare soil, and the snow cover fraction of the canopy was used to calculate the ground surface albedo. As in the equation (2),

$$\alpha_g = \left(1 - f_{snow,g}\right)\alpha_{soil} + f_{snow,g}\alpha_{snow} . \tag{2}$$

Where α_{soil} and α_{snow} are the albedo of bare soil and snow, respectively. $f_{snow,g}$ is the snow cover fraction on the ground and parameterized as a function of snow depth, ground roughness length and snow density (Niu and Yang, 2006).

https://doi.org/10.5194/hess-2022-350
Preprint. Discussion started: 17 October 2022

2.3 Genetic particle filter data assimilation scheme

The Bayesian recursive estimation problem is solved by the Monte Carlo approach within PF technique, making this scheme is appropriate for nonlinear models and various probability distributions (Magnusson et al., 2017). The main idea of PF technique is to use a large number of random realizations (i.e., particles) of the system state to represent the posterior distribution, at the same time, the particles are propagated forward in time as the model evolved. The weights associated with the particles are updated based on the likelihood of each particle's simulated proximity to the real observation, and the weight of the particles can be updated as follows:

$$w_t^i = w_{t-1}^i p\left(z_t \middle| x_t^i\right). \tag{3}$$

where w_{t-1}^i is the weight of i th particle at time $t-1$ and the weight is updated by the likelihood function $p\left(z_t \middle| x_t^i\right)$, the observation z_t of state variable is employed in this function. Usually, a Gaussian error distribution was considered to perturb the observation values and the likelihood function was defined to represent the errors. In this study, a normal probability distribution was employed to serve as likelihood function:

$$p\left(z_t \middle| x_t^i\right) = N\left(z_t - x_t^i, \sigma\right). \tag{4}$$

where N is the normal probability distribution of the residuals between the observed, z_t, and simulated, x_t. Finally, the weights of the updated state variable would be normalized, and the assimilated value of state variable is the weighted average of all particles at time t. Although the particle filter has a broad vision of application in nonlinear system, the particle degeneracy and impoverishment are still the limitations of particle filter. To overcome the degeneration problem in the PF algorithm, the resampling methods like multinominal resampling, systematic resampling, etc. were used to resample the particles if the effective sample size,

$$N_{eff} = 1 \Big/ \sum_{i=1}^{N} \left(w_t^i\right)^2. \tag{5}$$

fell below a specified number of particles. Although the particle degeneracy problem can be eliminated by the resampling methods, it can also make the particles lack of diversity. In this study, the genetic algorithm (GA) was chosen to resample the particles. The GA was inspired by Darwin's evolution theory and emphasizes the principle of the survival of the fittest, exactly, the fitness of particles should be chosen in the particle filtering phase. And the crossover and mutation operator can be used to produce better offspring to improve the whole population fitness, this can prevent sample impoverishment or a lack of particle diversity, especially when the processing noise is low. As shown in Figure 1, the effective ensemble size E_f was used to measure the degeneracy of the PF algorithm.

https://doi.org/10.5194/hess-2022-350
Preprint. Discussion started: 17 October 2022

Hydrology and Earth System Sciences
Discussions

The GA algorithm will be used to improve whole particles when $E_f < E_0$, and the procedure of GA can be divided into three steps: resample, crossover and mutation. First, the fitness of each particle was calculated and were then sorted in ascending order. Obviously, the fifth percentile of particles are fitness and be resampled. Second, the resampled particles were used to produce offspring by the crossover operator. Last, in order to increase the diversity of particles, the mutation operator was employed. A large number of particles may lead to filter collapse (Mechri et al., 2014), we set the number of particles to 100 in this study. To avoid the particle ensemble unable to represent the prior of state variable due to the structurally deficient within model operator, in this study, a model error of gaussian noise type based on experience was added to the ensemble members before assimilating the measurements.

2.4 DA experimental design

2.4.1 Perturbation of meteorological input data

The accuracy of model's output largely depends on the input meteorological forcing dataset for land surface models, and meteorological forcing are one of the major sources of uncertainty affecting simulation results (Raleigh et al., 2015). The precipitation and air temperature are the most important input elements for snow simulations since their roles in determining the quantity of rainfall and snowfall.

To produce the forcing data ensemble, the air temperature and precipitation were perturbed following the method of Lei et al. (2014). In this study, the precipitation was assumed to have an error with a log-normal distribution, and it is expressed as follows:

$$P_t^i = \exp\left(\mu_{\ln P} + \varphi_{P,i} \cdot \sigma_{\ln P} / 2\right). \tag{6}$$

$$\sigma_{\ln P} = \sqrt{\ln\left(\frac{\left(\alpha_p \cdot P_t\right)^2}{P_t^2} + 1\right)}. \tag{7}$$

$$\mu_{\ln P} = \ln\left(\frac{P_t^2}{\sqrt{P_t^2 + \left(\alpha_p \cdot P_t\right)^2}}\right). \tag{8}$$

where P_t and P_t^i are the observed and perturbed precipitation at time t, respectively; the log transformation of P_t^i is a Gaussian distribution with a mean ($\mu_{\ln P}$) and a standard deviation ($\sigma_{\ln P}$); α_P is the variance scaling factor of the precipitation, which was set to 0.5 in this study; and $\varphi_{P,i}$ is a normally distributed random number. The number of particles was set to 100 according to the sensitivity experiment by Magnusson et al. (2017). The ensemble of the air temperature was obtained

https://doi.org/10.5194/hess-2022-350
Preprint. Discussion started: 17 October 2022

Hydrology and Earth System Sciences
Discussions

as follows:

$$T_t^i = T_t - \gamma\left(1-2w^i\right), w^i \sim U\left(0,1\right). \tag{9}$$

where T_t and T_t^i are the observed and perturbed air temperatures at time t, respectively; γ is the variance scaling factor of the temperature with a value of 2.0; and w^i is the random noise with a uniform distribution between 0 and 1.

2.4.2 Evaluation metrics

In order to properly quantify the filter performance, each experiment is evaluated by statistical analysis based on the daily mean values of simulations and observations. In this paper, the filter performance was evaluated using the Kling-Gupta efficiency (KGE) coefficient (Gupta et al., 2009) allows the analysis of how the assimilation of snow observations succeeds in properly updating the model simulations, on average:

$$KGE = 1-\sqrt{\left(r-1\right)^2+\left(a-1\right)^2+\left(b-1\right)^2}. \tag{10}$$

Where r is the linear correlation coefficient between the simulated and observed SD; a is the ratio of the standard deviation of simulated SD to the standard deviation of the observed ones; and b is the ratio of the mean of simulated SD to the mean of observed ones, obviously, the simulated SD is the mean SD ensemble simulations in this paper. Theoretically, when $r=1$, $a=1$ and $b=1$ in formula (10), the KGE will obtain the optimal value which equal to 1, in this case, the simulated SD highly consistent with the observed ones.

To evaluate the performance of the assimilation, the time series of SD obtained from assimilation scenarios is compared to observations, and the root-mean-square error (RMSE) was employed:

$$RMSE = \sqrt{\frac{1}{N}\sum_{i=1}^{N}\left(obs(i)-sim(i)\right)^2}. \tag{11}$$

Where N is the total number of observations, $sim(i)$ is the simulated value at time i, $obs(i)$ is the observed value at time i.

Another statistical index employed as evaluation metric in this paper is the continuous ranked probability skill score (CRPSS), and the calculation scheme is shown in equation (12):

$$CRPSS = 1-\frac{CRPS}{CRPS_{ref}}. \tag{12}$$

Where CRPS is the continuous ranked probability score which can quantify the difference between continuous probability distribution and deterministic observation samples (detail in Hersbach, 2000). A smaller CRPS value indicates better probabilistic simulation and the CRPS score of a perfect simulation would equal to 0. Therefore, the changes in overall accuracy of the SD ensemble

https://doi.org/10.5194/hess-2022-350
Preprint. Discussion started: 17 October 2022

simulations can be measured by CRPSS, certainly, unlike the CRPS score, the optimal CRPSS score is equal to 1 and negative values indicate a negative improvement with respect to the reference ones.

3. Results and discussion

3.1 Open-loop ensemble simulations

To investigate the impact of meteorological perturbations, 100 ensemble snow depth simulations derived by as many different meteorological conditions are analyzed. For the sake of concision, a representative winter season was selected for each site and shown in Figure 2. As shown in Figure 2, the possible overestimation and underestimation of snow depth simulations produced by the perturbation forcing data were contained in the ensemble spread. And the ensemble simulations are the direct consequence of perturbation of the forcing data. Certainly, the nonlinearity of physical processes within model is the main reason for this issue under the condition of the meteorological perturbations are supposed to unbiased (Piazzi et al. 2018). During the winter season, precipitation and air temperature are primary factors which can determine the total amount of snow. As Figure 2 shows, the intervals of SD ensemble are significant different in distinct sites though an identical meteorological perturbation method was used. In some sites, like ATY, MOHE, WFJ and CDP, a larger SD ensemble interval was obtained and most of SD observations were covered by the uncertainty spread. However, in other sites, like in ROPA, SDA and SASP, a narrow SD ensemble interval was obtained and the SD uncertainty spread can hardly cover observations, especially in ROPA, we can hardly figure out any variation rules of snow depth and the snow cover was extremely unstable. The narrow SD ensemble spread in these sites demonstrated that the precipitation and air temperature are not the main factors causing snow change in these sites. Like in ROPA site, sublimation losses at ROPA ranged from 24% to 33% of total annual ablation and occurred 60% of the time during which snow was present, and high sublimation rate may be the main reason for snow instability (Herrero et al., 2016; You et al., 2020a). At all sites, it was found that the spread of SD ensembles is increased when a snowfall event occurred due to the perturbation in precipitation would providing different input snow rates for model realization. It was expected to obtain a SD ensemble spread which can cover or nearly cover SD observations at all sites using the meteorological perturbation method, however, at some sites, like SNQ, SDA, etc., the spread of SD ensembles was found has a seriously underestimation. On the one hand, the precipitation and air temperature are not the dominant factors affecting snow cover change which lead to a narrowed ensemble spread at these sites. On the other hand, though the variation trend of snow cover can be accurately expressed by Noah-MP model, seriously underestimation of the simulated SD shows the snow simulation performance of Noah-MP is poor at these sites. Certainly, despite this, the simulated ensembles will be improved whenever the model and observation error are considered.

https://doi.org/10.5194/hess-2022-350
Preprint. Discussion started: 17 October 2022

3.2 DA simulations with perturbed forcing data

In this study, the SD measurements were assimilated into Noah-MP model and the frequency of SD observation is 5 days. The SD assimilation results across snow climates are shown in Figure 3. It can be found that the GPF show a satisfactory assimilation performance at all sites, the SD simulations obtain a great improvement and closer to observations. Not only can the GPF algorithm solve the seriously underestimation, like at SNQ, SDA etc., but also the overestimation occurred during snow ablation period, such as at CDP, SASP, ATY and MOHE site, can be handled correctly. It was demonstrated that the GPF algorithm used as snow data assimilation scheme can make a substantial improvement for SD simulations despite seriously overestimation and underestimation occurred in Noah-MP model snow simulation results across snow climates.

With respect to the open-loop run, the KGE values of the SD simulations relying on the perturbed meteorological forcing data reveal the effectiveness of GPF in updating SD simulations, as shown in Figure 4. Although the mean ensemble simulations of SD show a substantial improvement at all sites, not all members were improved according to the distribution of KGE values. We found the ensemble members were actually obtained a substantial improvement at some sites, like SDA, SASP, MOHE and SNQ and a slight improvement at sites like ATY, WFJ. However, the update of SD model simulations at ROPA and WFJ site are more challenging. It was well known that the snow simulation performance of Noah-MP model was poor at ROPA site since the special weather condition. Certainly, the median value of SD ensemble prediction KGE values as expected below zero at this site, indicating that there are few qualified simulations in the prediction ensemble. Even though the GPF succeeds in enhancing the SD simulations at ROPA site, the distribution of GPF-DA KGE values is not concentrated enough. The 25th percentile approximately to 0.2 and the 75th percentile is about 0.7, more than half of ensemble members are below 0.5. This indicated that the GPF assimilation algorithm cannot enhance all members but it can raise the mean level and obtain an approximation of the optimal posterior estimation. Conversely, the update of SD model predictions is more challenging at CDP site, and CDP is the only site which the assimilation of snow measurements actually results in a poor quality of the SD simulations with respect to the open-loop ensemble simulations. As shown in Figure 4, the median value of GPF-DA KGE is less than the median value of OL KGE, this indicates that a considerable number of ensemble simulations fail in well catching the observed values after assimilating snow data. Nevertheless, we still found the mean ensemble simulations after assimilating snow data is much closer to SD observations in Figure 3. This explains that the ensemble mean is an important quantity to characterize the filter effectiveness and the practical value of the optimal posterior estimation of model state. Certainly, the scale of model ensemble spread is the determinant factor which have a profound effect on assimilation results. A large ensemble spread can adjust the simulations toward the observed system state even if the model predictions are heavily biased.

Figure 5 shows the CRPSS value of GPF-DA at different sites. The smaller the CRPSS value,

https://doi.org/10.5194/hess-2022-350
Preprint. Discussion started: 17 October 2022

the worst the probabilistic simulation (the optimal score being equal to 1). The CRPSS at SASP gets the maximum value 0.91, and the lowest score is 0.44 at CDP site. That indicates the GPF enhance the overall accuracy of the ensemble simulations most at SASP site and least at CDP site with respect to the open-loop ensemble simulation. Certainly, this cannot be illustrated by the mean ensemble simulations (Figure 3) but consistent with the KGE statistical results (Figure 4). Even though the open-loop simulations at SNQ site show a very serious underestimation, a satisfactory assimilation result was obtained at this site and the CRPSS score is 0.87. At SNQ site, the snow simulation performance of Noah-MP model is poor and shows a seriously underestimation during snow stable phase, implementing data assimilation experiment in this case is a tricky business since it is very difficult to obtain a suitable simulated ensemble by perturbing the meteorological forcings. However, due to the model error and observation error are considered in GPF algorithm, the overall accuracy of the ensemble simulations will be substantial enhanced and this the reason why it can obtain a satisfactory assimilation result at SNQ site. It is not easy to enhance the overall accuracy of the ensemble simulations at ROPA, the CRPSS score is 0.58 at this site. The snow cover was extremely unstable and the variation in snow depth exhibited extreme irregularity may be the main obstacles to snow data assimilation at this site.

Based on the above analysis, we concluded that the effectiveness of GPF varied among snow climates: it can be employed as snow data assimilation scheme across snow climates, however, it showed different performance at different sites. It is necessary to explore the sensitivity of measurement frequency and ensemble size to snow data assimilation scheme for different sites.

3.3 Sensitivity analysis of DA scheme to SD measurement frequency

With the aim of investigating the performance of GPF to SD measurement frequency, the sensitivity experiment was conducted at the eight sites to assess how the reduction of SD observed data affects the DA simulations. Obviously, a reduction in SD measurement frequency is expected to reduce the impact of the GPF updating on the model simulations, and the RMSE mean value gradually increased. Figure 6 shows the RMSE ensembles of snow depth simulations resulting from the assimilation of different frequency SD observations throughout the snow period at all sites. Obviously, assimilating higher frequency of SD observations is more helpful to improve the effectiveness of GPF, like the frequency of SD observation equals to 5 days, the ensemble simulations obtain lower RMSEs at all sites. Certainly, the range of RMSE values at different sites have a significant difference since it relates to the maximum snow depth, for instance, a thick snow at SNQ and WFJ site during the snow period lead to larger RMSEs of snow depth simulations. As shown in this figure, it is noteworthy that an increase in the length of assimilation window generally result in a significant increment of the simulation RMSE. Certainly, an abnormal situation occurred at SDA site, the assimilation effect of 20 days SD observations is significantly better than the assimilation effect of 15 days SD observations. Actually, despite the RMSE distribution of SD assimilation result with 20 days observations seems superior to the assimilation result with 15 days, however, the RMSE mean value of the two are very close, one is 0.08 m and the other is 0.07 m. Therefore, this anomaly can be ignored. It indicates that the frequency of SD observations has a significant impact on the effectiveness of GPF algorithm, and a dense observation data can effectively improve the assimilation result.

3.4 Sensitivity analysis of DA scheme to ensemble size

The main results of the experiment aiming to evaluate the impact of particle number on the assimilation performance of GPF is shown in Figure 7. As expected, an increase in the particle number which less than threshold generally result in a significant increment of the percent effective sample size. However, the filter performance is not significantly improved when the particle number greater than the threshold. Figure 7 shows that the GPF would get the minimum error at all sites when the particle number is 100, and one hundred particles can optimize the performance of GPF algorithm. Although large particle number can enhance particle diversity and prevent filter divergence, it will increase the computation burden, and this cannot reduce the error of the system. As shown in Figure 7, the RMSEs are basically at the same level when the particle number equals to 120 and 160, and the RMSE is significantly larger than the RMSE when the particle number is equal to 100. A low system sensitivity to the ensemble size is also clearly proven by the slight impact of the change in the particle number on the performance of GPF when the particle number is less than the threshold, and this has been occurred at all sites. Essentially, the increase of the particle number does not ensure a better DA performance of GPF algorithm. As shown in Figure 7, although the particle number increased from 120 to 160, the RMSEs of simulated snow-depth are basically unchanged at all sites. It indicates that a blindly increasing ensemble size is futile to improve the performance of GPF, it just can increase the computational burden.

4. Conclusions

This study investigated the potential of GPF used as a snow data assimilation scheme at eight sites across different snow climates. To solve the problem of degeneration and impoverishment in PF algorithm, we used the genetic algorithm to resample particles when the particle threshold is below 0.95. On this basis, we examined the sensitivity of GPF scheme to measurement frequency and ensemble size. The main findings of this study are as follows.

1. The GPF was an effective snow data assimilation scheme and can be used across different snow climates. The genetic algorithm can effectively solve the problem of particle degeneration and impoverishment in PF algorithm.
2. In this point-scale application of the ground SD measurement, the system has revealed a low sensitivity to the particle number, thereby proving that 100 particles can be obtained a better assimilation result across different snow climates, that is, 100 particles can be suited to represent

the high dimensionality of the system.

3. The perturbation of the meteorological forcing data has turn out not to be sufficient for providing ensemble spread and resulting a poor filter performance. However, particle inflation can make up for this deficiency. The RMSE of simulated SD would decrease significantly with the increase of the frequency of SD measurement, that is, a dense observational data can dominate the assimilation results.

The experiments conducted in this paper were based on forcing data and snow observations from the sites across different snow climates. On the one hand, the performance of the GPF on the regional scale is needed to be investigated; on the other hand, additional studies are need to explore the snow observational data which from remote sensing or wireless sensor network assimilated into LSM by GPF. Overall, the results of this study providing a reference for applying the GPF to snow data assimilation and the feasibility of GPF across different snow climates has been proved.

Acknowledgements

This work was supported by the National Natural Science Foundation of China (grant number 42101361, 42130113, 41871251 and 41971326).

References

Abbasnezhadi, K., Rousseau, A. N., Foulon, E., et al. (2021), Verification of regional deterministic precipitation analysis products using snow data assimilation for application in meteorological network assessment in sparsely gauged Nordic basins, Journal of Hydrometeorology, 22(4): 859-876.

Abbaszadeh, P., Moradkhani, H., Yan, H. X. (2017), Enhancing hydrologic data assimilation by evolutionary particle filter and Markov Chain Monte Carlo, Advances in Water Resources, 111: 192-204.

Barnett, T. P., Adam, J. C., Lettenmaier, D. P. (2005), Potential impacts of a warming climate on water availability in snow-dominated regions, Nature, 438(7066): 303-309.

Balsamo, G., Albergel, C., Beljaars, A., et al. (2015), ERA-Interim/Land: a global land surface reanalysis data set, Hydrology and Earth System Sciences, 19(1): 389-407.

Chen, Z. (2003), Bayesian filtering: From Kalman filters to particle filters, and beyond, Statistics, 182(1): 1-69.

Cortes, G., Girotto, M., Margulis, S. (2016), Snow process estimation over the extratropical Andes using a data assimilation framework integrating MERRA data and Landsat imagery, Water Resources Research, 52(4): 2582-2600.

Dee, D. P., Uppala, S. M., Simmons, A. J., et al. (2011), The ERA-Interim reanalysis: configuration and performance of the data assimilation system, Quarterly Journal of the Royal Meteorological Society, 137(656): 553-597.

https://doi.org/10.5194/hess-2022-350
Preprint. Discussion started: 17 October 2022

Dechant, C., Moradkhani, H. (2011), Radiance data assimilation for operational snow and streamflow forecasting, Advances in Water Resources, 34(3): 351-364.

Dettinger, M. (2014), Climate change impacts in the third dimension, Nature Geoscience, 7(3): 166-167.

Gelb, A. (1974), Optimal linear filtering, in: Applied optimal estimation, MIT Press, Cambridge, Mass, 102-155.

Griessinger, N., Seibert, J., Magnusson, J., et al. (2016), Assessing the benefit of snow data assimilation for runoff modeling in Alpine catchments, Hydrology and Earth System Sciences, 20(9): 3895-3905.

Hersbach, H. (2000), Decomposition of the continuous ranked probability score for ensemble prediction systems, Weather and Forecasting, 15(5): 559-570.

Kwok, N., Fang, G., Zhou, W., (2005), Evolutionary particle filter: resampling from the genetic algorithm perspective. In: Proceedings of International Conference on Intelligent Robots and Systems, Shaw Conference Centre, Edmonton, Alberta, Canada, August 2-6, pp. 2935-2940.

Mechri, R., Ottle, C., Pannekouche, O., et al. (2014), Genetic particle filter application to land surface temperature downscaling, Journal of Geophysical Research-Atmospheres, 119(5): 2131-2146.

Magnusson, J., Gustafsson, D., Husler, F., et al. (2014), Assimilation of point SWE data into a distributed snow cover model comparing two contrasting methods, Water Resources Research, 50(10): 7816-7835.

Margulis, S. A., Girotto, M., Cortes, G., et al. (2015), A particle batch smoother approach to snow water equivalent estimation, Journal of Hydrometeorology, 16(4): 1752-1772.

Magnusson, J., Winstral, A., Stordal, A. S., et al. (2017), Improving physically based snow simulations by assimilating snow depths using the particle filter, Water Resources Research, 53(2): 1125-1143.

Moradkhani, H., Hsu, K. L., Gupta, H., et al. (2005), Uncertainty assessment of hydrologic model states and parameters: Sequential data assimilation using the particle filter, Water Resources Research, 41(5): W05012.

Mechri, R., Ottle, C., Pannekoucke, O., et al. (2014), Genetic particle filter application to land surface temperature downscaling, Journal of Geophysical Research-Atmospheres, 119(5): 2131-2146.

Niu, G. Y., Yang, Z. L. (2006), Effects of frozen soil on snowmelt runoff and soil water storage at a continental scale, Journal of Hydrometeorology, 7(5): 937-952.

Oaida, C. M., Reager, J. T., Andreadis, K. M., et al. (2019), A high-resolution data assimilation framework for snow water equivalent estimation across the western United States and validation with the airborne snow observatory, Journal of Hydrometeorology, 20(3): 357-378.

Park, S., Hwang, J. P., Kim, E., et al. (2009). A new evolutionary particle filter for the prevention of sample impoverishment, IEEE Transaction on Evolutionary Computation, 13(4): 801-809.

Parrish, M. A., Moradkhani, H., DeChant, C. M. (2012), Toward reduction of model uncertainty: Integration of Bayesian model averaging and data assimilation, Water Resources Research, 48:

W03519.

Piazzi, G., Campo, L., Gabellani, S., et al. (2019), An EnKF-based scheme for snow multivariable data assimilation at an Alpine site, Journal of Hydrology and Hydromechanics, 67(1): 4-19.

Piazzi, G., Thirel, G., Campo, L., et al. (2018), A particle filter scheme for multivariate data assimilation into a point-scale snowpack model in an Alpine environment, Cryosphere, 12(7): 2287-2306.

Smyth, E. J., Raleigh, M. S., Small, E. E. (2020), Improving SWE estimation with data assimilation: the influence of snow depth observation timing and uncertainty, Water Resources Research, 56(5): e2019WR026853.

Su, H., Yang, Z. L., Niu, G. Y., Dickinson, R. E. (2008), Enhancing the estimation of continental-scale snow water equivalent by assimilating MODIS snow cover with the ensemble Kalman filter, Journal of Geophysical Research-Atmospheres, 113(D8): D08120.

Takala, M., Luojus, K., Pulliainen, J., et al. (2011), Estimating northern hemisphere snow water equivalent for climate research through assimilation of space-borne radiometer data and ground-based measurements, Remote Sensing of Environment, 115(12): 3517-3529.

Weerts, A. H., El Serafy, G. Y. H. (2006), Particle filtering and ensemble Kalman filtering for state updating with hydrological conceptual rainfall-runoff models, Water Resources Research, 42(9): W09403.

Yang, J. M., Li, C. Z. (2021), Assimilation of D-InSAR snow depth data by an ensemble Kalman filter, Arabian Journal of Geosciences, 14(6): 505.

Zhang, T. J. (2005), Influence of the seasonal snow cover on the ground thermal regime: An overview, Reviews of Geophysics, 43(4): 1-23.

https://doi.org/10.5194/hess-2022-350
Preprint. Discussion started: 17 October 2022

Hydrology and Earth System Sciences
Discussions

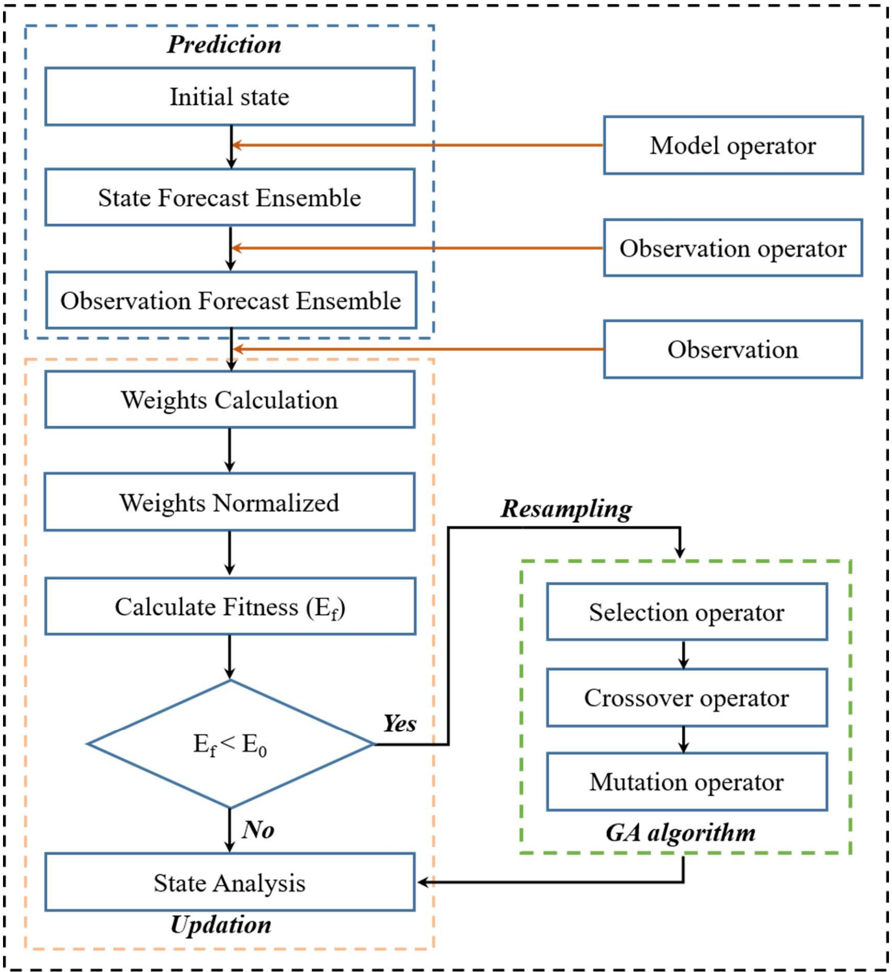

Figure 1. Flowchart of Genetic particle filter

https://doi.org/10.5194/hess-2022-350
Preprint. Discussion started: 17 October 2022

518
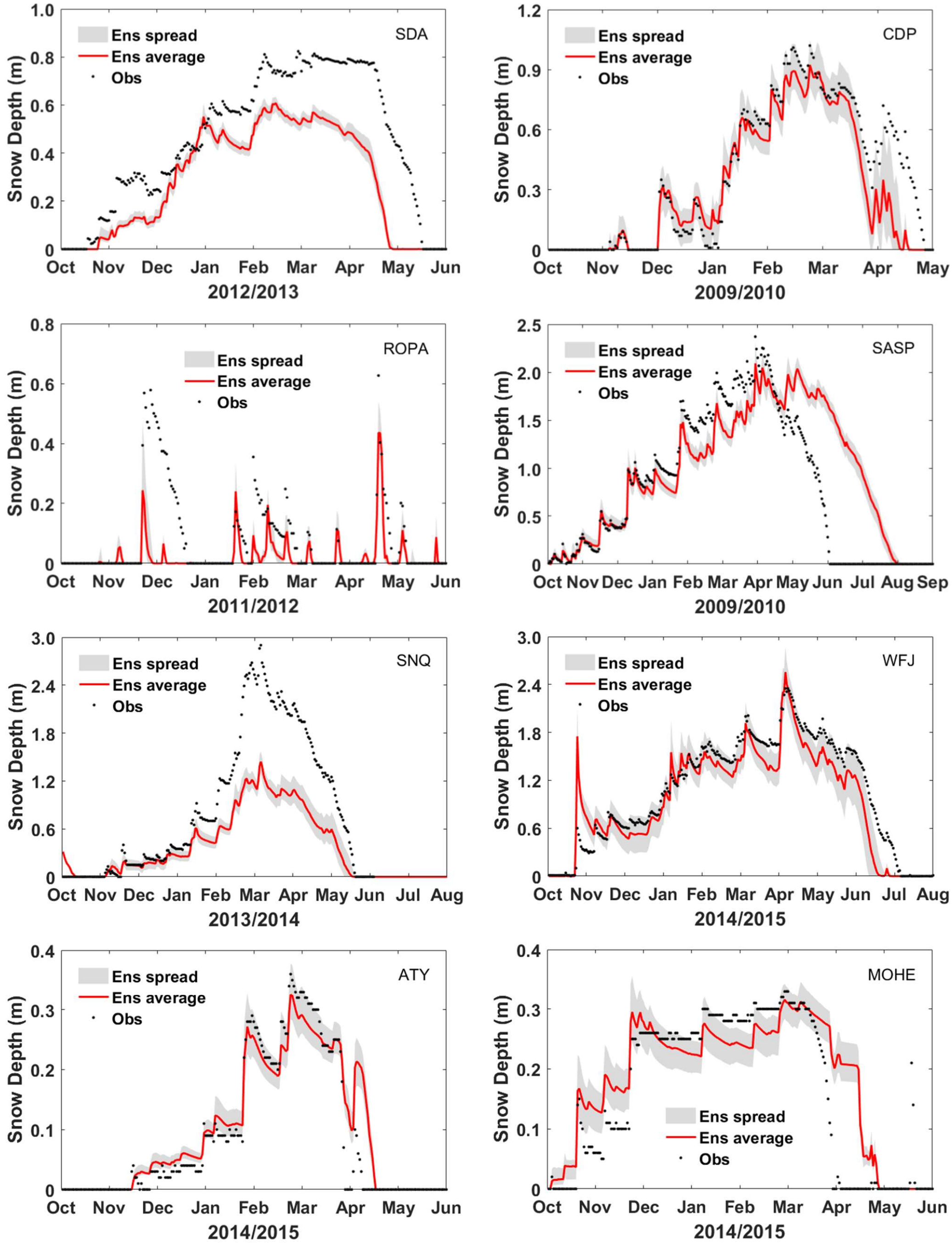

519 **Figure 2.** Impact of the meteorological uncertainty on snow depth ensemble simulations

520

https://doi.org/10.5194/hess-2022-350
Preprint. Discussion started: 17 October 2022

Hydrology and Earth System Sciences
Open Access
Discussions

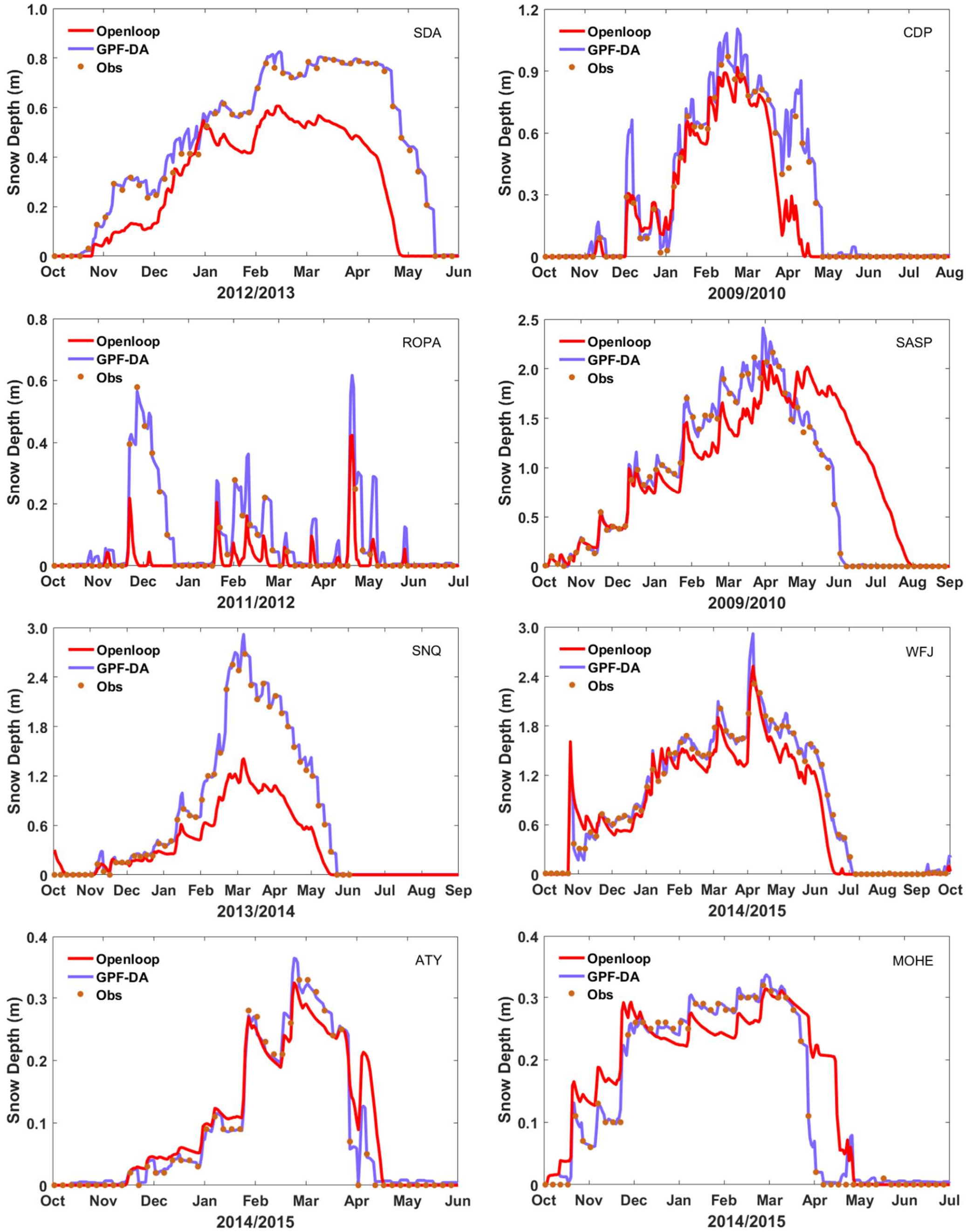

Figure 3. Evaluation of the SD at eight sites from mean ensemble simulation and assimilation with the measurements.

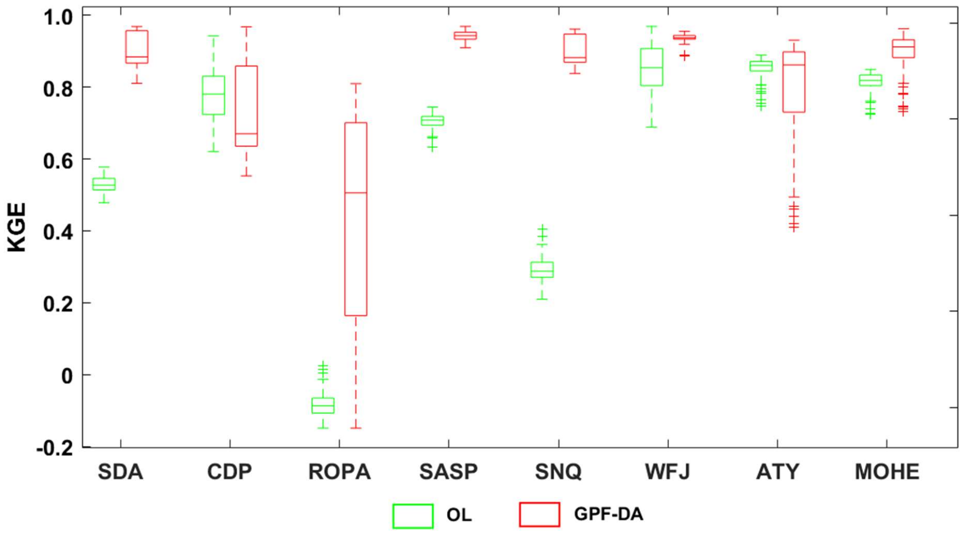

Figure 4. The KGE values of SD simulations, the OL and GPF-DA are in green, red, respectively. The bottom and top edges of each box indicate the 25th 75th percentiles, respectively. The line in the middle of each box is the median.

https://doi.org/10.5194/hess-2022-350
Preprint. Discussion started: 17 October 2022

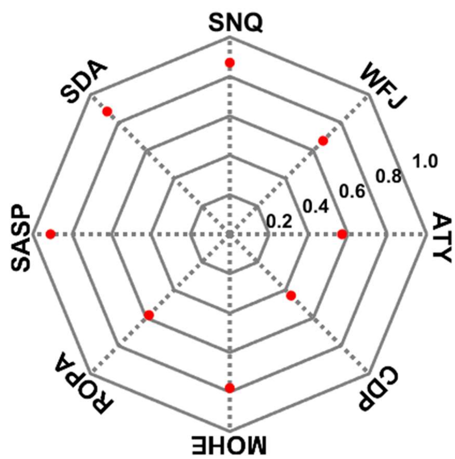

Figure 5. Comparison of the CRPSS value of GPF-DA at different sites.

https://doi.org/10.5194/hess-2022-350
Preprint. Discussion started: 17 October 2022

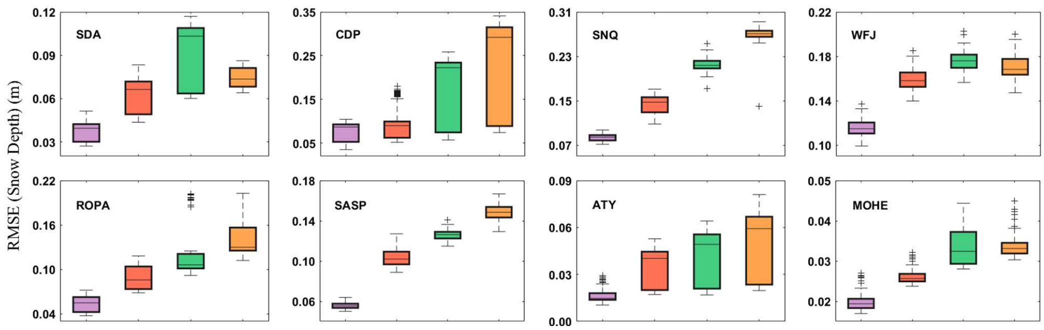

Figure 6. The RMSE values of SD simulations at different sites, from left to right in each subfigure are the assimilation observation frequency is 5, 10, 15, 20 days, respectively, and with different colors.

https://doi.org/10.5194/hess-2022-350
Preprint. Discussion started: 17 October 2022

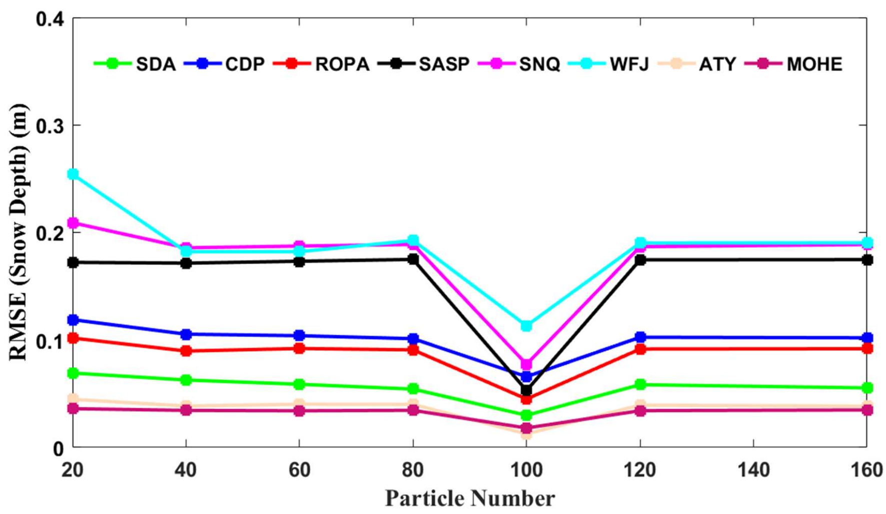

Figure 7. Sensitivity analysis of the GPF snow DA scheme to particle number at eight sites, during different snow periods.